A small angle neutron scattering study of the spin-glass $Fe_{90}Nd_3Zr_7$ amorphous alloy

2008 J. Phys.: Condens. Matter 20 104219

(http://iopscience.iop.org/0953-8984/20/10/104219)

J. Phys.: Condens. Matter **20** (2008) 104219 (6pp) doi:10.1088/0953-8984/20/10/104219

A small angle neutron scattering study of the spin-glass $Fe_{90}Nd_3Zr_7$ amorphous alloy

K Mergia and S Messoloras

Institute of Nuclear Technology and Radiation Protection, National Centre for Scientific Research 'Demokritos', GR15310 Aghia Paraskevi Attikis, Greece

Received 27 July 2007, in final form 10 September 2007
Published 19 February 2008
Online at stacks.iop.org/JPhysCM/20/104219

Abstract

The spin-glass state of the amorphous alloy $Fe_{90}Nd_3Zr_7$ has been studied by small angle neutron scattering. Irreversibility between zero-field cooling and warming up appears at around 200 K and below. During cooling down a sharp transition appears at 188 K, whereas on warming up the transition at the same temperature is smooth. From the analysis of the data is concluded that, below the transition temperature, the system breaks up into regions having a multitude of transition temperatures. The scattering is attributed to the interaction among the different regions as they attempt to undergo a ferromagnetic transition in competition with each other.

1. Introduction

The re-entrant spin-glass (RSG) transition is a well known phenomenon of spin glasses (SGs) [1]. With decreasing temperature the magnetization increases; it then ceases at a lower temperature. At a much lower temperature, the spin-glass state (SG) characterized by ferromagnetic (FM) clusters is attained. It is thought that the system decomposes into an FM part and an SG system of frustrated spins [2]. Evidence of decomposition into two parts is given by a number of quasielastic and inelastic neutron experiments [3]. The SG part is concentrated in domains with a lower spin concentration which are weakly ordered at lower temperatures under the influence of the FM part. At even lower temperatures the SG part freezes and the FM part breaks up into FM clusters. Between the SG and the FM regions there is an interface [4]. 'True re-entrance' to the RSG phase without the long-range FM order cannot occur in the mean-field models [5, 6].

Amorphous Fe–Zr alloys have been investigated through various experimental techniques in order to understand these phenomena [7]. From experimental studies a number of different pictures of the SG state have emerged as antiferromagnetic Fe clusters in an FeZr matrix, an FM state with transverse SG ordering, an infinite 3D FM network and finite freezing at random spin clusters [8–10]. The replacement of Fe in Fe rich Fe–Zr alloys by any transition metal brings out dramatic changes in their magnetic behaviour [11, 12].

In this work part of the Zr in the system $Fe_{90}Zr_{10}$ studied previously with SANS [13] has been replaced with Nd, i.e. the amorphous alloy $Fe_{90}Nd_3Zr_7$ is studied. The localization of the Nd states is expected to modify the RKKY interactions and thus to enable a better understanding of the RSG phenomena. For the study of the magnetic state of this amorphous alloy we employ small angle neutron scattering (SANS) measurements, as it is a suitable technique to measure the susceptibility of the sample in zero magnetic field, i.e. it is a probe of the ground state of the system. Looked at from another angle SANS can give information on the long-range magnetic structure which in our opinion forms the basis in understanding the complex dynamic phenomena or magnetic field induced changes of the SG systems.

2. Small angle neutron scattering from spin glasses

The scattering from a magnetic system is described by its spin–spin correlation function $g(r)$ (isotropic system) which can be separated into two parts, the one describing the long-range correlations $g_{\rm lr}(r)$ and the other the short-range ones $g_{\rm sr}(r)$. The neutron scattering is then given by

$$S(Q) = F\{g_{\rm lr}(r)\} + F\{g_{\rm sr}(r) - \langle g(r)\rangle\}, \qquad (1)$$

where $F\{\}$ denotes the sine Fourier transform, i.e.

$$F\{g(r)\} = \frac{1}{A}\int g(r)r^2\frac{\sin Qr}{Qr}\,{\rm d}r, \qquad A = \int g(r)r^2\,{\rm d}r. \qquad (2)$$

$\langle g(r)\rangle$ is the averaging over the whole sample volume and $|\mathbf{Q}| = 4\pi\sin\theta/\lambda$ (2θ is the scattering angle and λ is

the neutron wavelength). The first term in equation (1) gives the scattering at high Q values (Bragg scattering in a polycrystalline sample), whereas the second term corresponds to SANS scattering. As the scattering is conserved, loss of scattering from the SANS region implies that the short-range order has been transformed to a long-range one (within the term long range is included the scattering from constant magnetization). Notwithstanding that in the low Q region the length scale observed is of the order $Qd \sim 2\pi$, abrupt changes in the observed scattering indicate transition to long-range order, whereas absence of them that the system has not undergone a long-range order transition (e.g. from paramagnetic to FM).

In the spin-glass case two types of correlation functions have been used and the scattering law is given by their sine Fourier transforms as

$$\begin{aligned} \frac{A}{r}\exp(-\kappa r) &\Leftrightarrow \frac{A\kappa^2}{\kappa^2+Q^2}\ (\mathrm{Lor}), \\ B\exp(-\kappa r) &\Leftrightarrow \frac{B\kappa^4}{(\kappa^2+Q^2)^2}(\mathrm{Lor}^2). \end{aligned} \tag{3}$$

Both Lor and Lor^2 curves can be easily distinguished from the usual Guinier approximation at low Q values which is applicable for objects having sharp interfaces with the surrounding matrix. The correlation length, ξ, given by $\xi = 1/\kappa$ might be different for the Lor or Lor^2 functions.

In a system in which random fields exist, the correlation function can be described by [14–16]

$$\langle \mathbf{S}_i(0) \circ \mathbf{S}_j(\mathbf{r})\rangle_{\mathrm{T}} \sim \frac{1}{r^{(d-3)/2}}\exp(-\kappa r), \tag{4}$$

where d is the dimensionality of the system. This correlation function for $d = 3$ gives the Lor^2 and a Lor + Lor^2 scattering law for lower dimensionalities. The form of the correlation function has recently attracted new attention [17].

3. Experimental details

Initially, a polycrystalline alloy $Fe_{90}Nd_3Zr_7$ was fabricated by arc melting. Amorphous ribbons were produced by fast cooling of the alloy on a rotating wheel, giving a cooling rate of 10^6 K s^{-1}, and in an argon atmosphere. The thickness of the produced ribbons was 10 μm and their width around 3 mm, exhibiting high elasticity consistent with their amorphous state. In addition XRD measurements showed no crystallinity. The SANS measurements were carried out at the LOQ instrument at the ISIS Neutron Spallation Source facility, in the UK.

In this work we shall discuss two types of experimental procedures, the one referred to as ZFC and the other as ZFW. In the first (ZFC) the sample was cooled down from room temperature to 30 K at a rate of 1.5 K min^{-1}; subsequently, the sample was further cooled to 8.5 K and then it was slowly warmed up to room temperature with a rate of 5 K min^{-1} (ZFW). In both cases SANS spectra were recorded continuously.

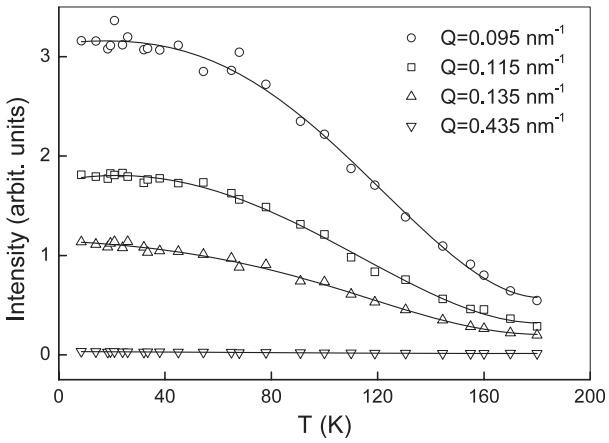

Figure 1. SANS for ZFW versus temperature for different values of Q.

4. Results and discussion

The scattering at room temperature is much lower than that observed at lower temperatures, and in contrast to the alloy $Fe_{90}Zr_{10}$ does not change with the application of a 1.2 T magnetic field [13]. Further, irrespective of any temperature or magnetic field path, the scattering at room temperature always returns to its initial value. From these results we can conclude that the scattering at room temperature can be attributed to chemical disorder and as such has been subtracted from the SANS measured at lower temperatures in order to derive the scattering of magnetic origin.

During cooling down to the temperature of 200 K the scattering remains almost constant. Below this temperature the scattering increases for $Q < 0.8$ nm^{-1}, whereas for larger Q values it remains constant. At 140 K there is an abrupt change in the scattering and then a continuous increase is observed down to 30 K. On warming up the scattering remains constant up to about 50 K and subsequently is quickly reduced up to 150 K. These changes in the scattering are mainly observed for Q values lower than 0.44 nm^{-1} and are depicted in figure 1. From this descriptive presentation of the SANS data it is apparent that below 200 K there is a magnetic structural change of the sample, and further a strong irreversibility between cooling down and warming up is observed.

In both cases of ZFC and ZFW the scattering above 200 K is described by a Lor function (see equation (3)), whereas below 200 K it is described by the sum of Lor and Lor^2 (Lor + Lor^2). This behaviour is shown in figure 2. From a least squares fit to the data of either Lor or Lor + Lor^2 functions, the parameters A, B and κ were determined. Wherever a Lor + Lor^2 function was employed, it was found that only one value of κ was needed to fit the data.

In figure 3 the correlation length, ξ, versus temperature for the ZFC data is presented. The data show a sharp FM type transition at around 200 K. This transition can be described by the scaling function

$$\xi(T, T_c) = \xi_0 \left| \frac{T}{T - T_c} \right|^{\nu}, \tag{5}$$

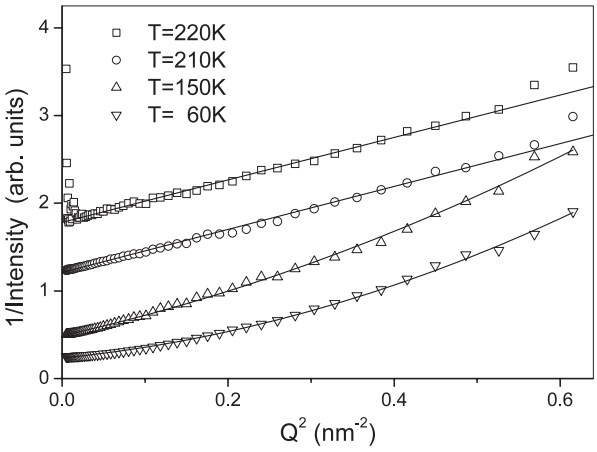

Figure 2. Inverse of the scattering $(1/S(Q))$ versus Q^2 for different temperatures with their least squares fitted curves (Lor for temperatures 220 and 210 K and Lor + Lor^2 for temperatures 150 and 60 K).

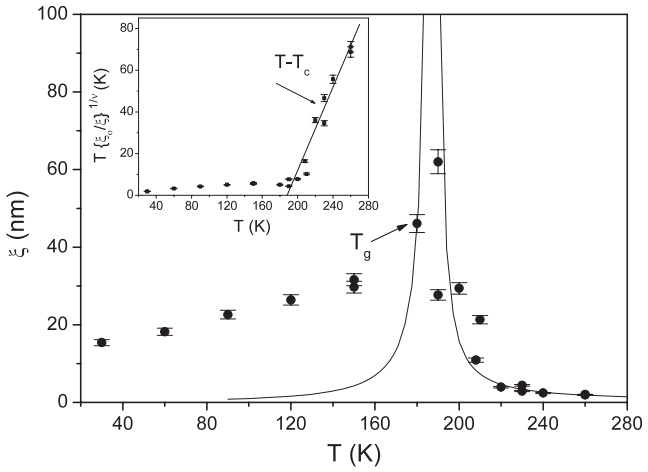

Figure 3. ZFC correlation length versus temperature. Line according to equation (5). Inset: $T(\xi_0/\xi)^{1/\nu}$ versus temperature, where $\nu = 1.4$.

where $\xi_0 = 0.31$ nm, $\nu = 1.4$ and $T_c = 188$ K. The applicability of the power law is better illustrated in the inset of figure 3, where the values of $T(\xi_0/\xi)^{1/\nu}$ versus temperature have been plotted. For a true FM transition and for temperatures below T_c, the short-range correlations observed by SANS are expected to lessen ($\xi \to 0$) and long-range order to be established, giving scattering at Bragg positions or high Q values for an amorphous system. From figure 3 we observe that the short-range correlations remain after a glass transition temperature at $T_g = 179$ K. Therefore, we cannot be quite sure that the sharp transition described by equation (5) really occurs and consequently that a long-range order has been established. Further, the glass transition temperature defined above should not be taken as defining a transition of the system breaking from a long-range order to regions of short-range order, as such a conjecture has to be proven. The next paragraphs are focused on interpreting the temperature dependence of the correlation length below the so called glass transition temperature.

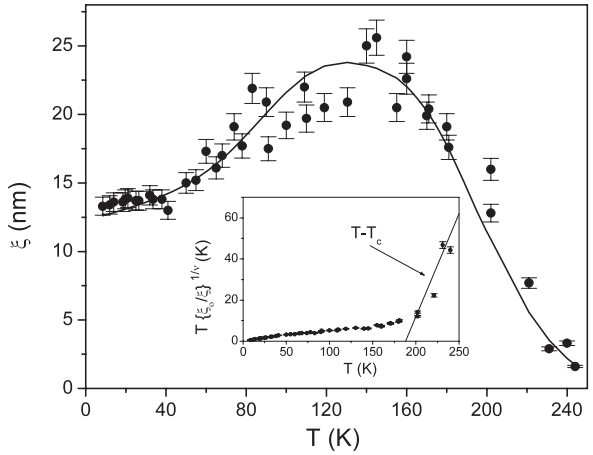

Figure 4. ZFW correlation length versus temperature. The continuous line is given by the equation $\xi = 23.0$ nm $\exp\{-|(T - 140\ \text{K})/70\ \text{K}|\}^{2.4} + 12.5$ nm $\exp\{-|(T - 20\ \text{K})/75\ \text{K}|\}^{2.4}$. Inset: $T(\xi_0/\xi)^{1/\nu}$ versus temperature, where $\nu = 1.4$.

At T_g there are regions with correlation lengths at around 50 nm. It is obvious that these regions are magnetic in origin since their correlation length is reduced with temperature. These regions need not to be static, as SANS results are a time average over all the whole sample volume. They, thus, can be thought of as long wavelength perturbations of the sample magnetization. However, if in each region we assign an average exchange coupling constant, different than the neighbouring ones and consequently different transition temperature $T_{c'}$, then a static picture of these regions emerges. In this picture the multitude of average exchange constants is attributed to chemical disorder, which results in a specific spin configuration in each region. Further, in order to be able to observe these regions with SANS, it is implied that these regions have different magnetization density than the average one, i.e. there is contrast (see equation (1)).

As there is a multitude of regions with different transition temperatures, what we observe below T_g is a transition of these regions to FM order or their attempt to reach long-range FM order. We can express this multitude of transitions as

$$\langle \xi(T) \rangle = \xi_0 \int n(T_{c'}) \xi(T, T_{c'})\, \mathrm{d}T_{c'}$$
$$= \xi_0 T \int n(xT) |1 - x|^{-\nu}\, \mathrm{d}x, \qquad (6)$$

where $\xi(T, T_{c'})$ is given by equation (5) and $n(T_{c'})$ is the distribution of the transition temperatures. Since we do not observe any poles in the correlation length versus temperature (see figures 3 and 4) we have to accept that the distribution of the transition temperatures is wide (or that $\xi(T, T_{c'})$ has no poles). This assumption implies that the number of states having $T_{c'}$ around T is small, and as with SANS we cannot observe very long correlation lengths the lack of any sharp transitions below T_g is understood. Assuming, at first, that there is no $1/T_{c'}$ dependence of $n(T_{c'})$, then the average correlation length according to equation (6) should vary linearly with T. This overall linear dependence is verified in figures 3 and 4 (below 130 K). However, the correlation

length does not go to zero as expected from equation (6) but to a constant value $\xi(0)$ of around 12 nm.

One could assign the $\xi(0)$ to regions which have exchange coupling constants such as that no long range could be established even at the lowest temperature applied. This interpretation would imply that, for example, at $T = 160$ K we have two sources of scattering, one arising from regions undergoing a transition with $\xi = 26$ nm and another from regions having a correlation length of $\xi(0)$ (see figure 3). If we generate a cross section as the sum of two Lorentzian functions corresponding to these ξ values and we analyse it according to figure 2, we find one ξ with a value close to 12 nm (in this averaging we assume that the values of A do not depend strongly on ξ). From this we conclude that the assumption of two types of regions is not correct. Equation (6) will result in a value of the correlation length different from zero as the temperature goes to zero only if the density of $T_{c'}$ states varies as

$$n(T_{c'}) \sim \frac{f(T_{c'})}{T - T_{c0}} \tag{7}$$

i.e. the number of states increases as we approach T_{c0} and below this it remains constant.

The discussion above can lead us into developing a picture of what happens. At a given temperature T, regions having $T_{c'}$ close to T attempt to grow. As they grow they find regions with lower $T_{c'}$ and their growth is limited by their neighbouring regions. As the temperature is lowered further, the number of possible states increases and thus the number of adjacent states having lower $T_{c'}$ values. This results in a reduction of the correlation length at lower temperatures. At around T_{c0} the number of available states is large and this imposes the limiting value of $\xi(0)$. Below T_{c0} the number of states remains constant and there is no change of the correlation length. This can be seen in figure 4, which sets $T_{c0} \sim 50$ K.

As the temperature increases from 10 K, a linear increase in ξ is observed with temperature (see figure 4) and the values of ξs in the ZFW are not different from those measured in the ZFC experiment. At around 160 K there is no further increase of the correlation length and at higher temperatures it starts decreasing. This observation demonstrates that at around 160 K the transformation starts to the paramagnetic state. This transition follows equation (5) with the same values of the constants (see the inset of figure 4). The cusp of the FM to paramagnetic state transition is not observed. Further, we have no indication that a part of the system, which might be assumed to be in a long-range FM state, undergoes an FM transition. These two observations put into doubt the picture of the co-existence of the SG and the long-range FM state.

Figure 4 can be interpreted in another way. We may assume that there is a range of transition temperatures assigned to different regions as above. As the temperature approaches the $T_{c'}$ of a given region, the correlation length of this region increases. As the temperature is further reduced, the region attempts to grow but the adjacent regions form a barrier to its growth and thus its size is reduced. This picture is quite similar to that described above. These types of transitions are not sharp, therefore can be described by a function of the form

$$\langle \xi \rangle = \xi_1 \exp\left(-\left|\frac{T - T_{c0}}{\Delta T}\right|^a\right). \tag{8}$$

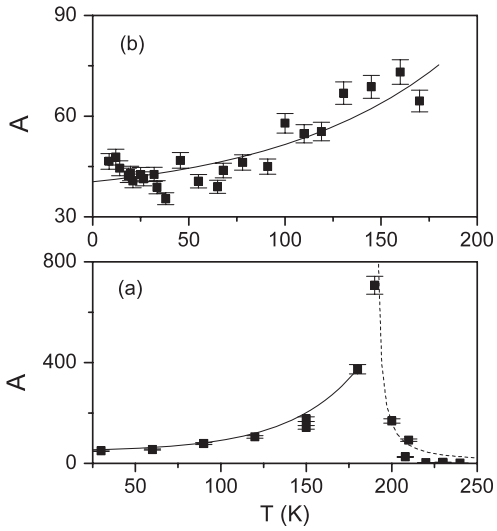

Figure 5. Coefficient A of the Lor function versus temperature. (a) ZFC. Dashed line: equation (5). Continuous line: $A = A_0 + A_1 \exp\{-(188\text{ K} - T)/40\text{ K}\}$. (b) ZFW. Continuous line $A = A_0 + A_1 \exp\{-(188\text{ K} - T)/90\text{ K}\}$.

The continuous line in figure 4 has been fitted to the data using the above assumption. We find that we need two distributions, one centred at $T_{c0} = 140$ K and the other at lower temperature at around 20 K. Both these distributions are quite wide. We also find that $a = \nu + 1$ (attempts to fit the data with smaller values of a have failed), which in some way implies that equation (8) is a type of integration of equation (5). One might suppose that the transitions we are referring to are transitions to a long-range FM state. In this case we would expect that a large part of the sample at low temperatures would be in the FM state. In this case its transition from FM state to paramagnetic, as the temperature is increased, should have been observed at 188 K. The smoothness of the data in figure 4 does not show that such a transition takes place.

The coefficients of the Lor functions for both cases of ZFC and ZFW are depicted in figure 5. In these coefficients, below 180 K, we do not observe the situation described by equation (8). We observe an exponential decay centred at the transition temperature $T_c = 188$ K. This might imply that the correlation function connected with the Lor part of the scattering characterizes the attempts of the system to go to a long-range FM order.

The Lor^2 function coefficients for ZFC and ZFW are plotted in figure 6. It should be remembered that the Lor^2 dependence of the scattering appears below the T_c of 188 K. For the Lor^2 coefficients we have a similar behaviour to that given by equation (8) (see figure 6). The low temperature $T_{c'}$ distribution does not appear in the ZFW case and this is probably because there are not many data points, especially at lower temperatures. Another point worth mentioning is that the B coefficient of the Lor^2 function is about 30 times larger than the A coefficient of the Lor. Intuitively we may assign the correlation function giving the Lor^2 scattering law to the interaction of the surfaces of the regions, as they attempt to grow. In a way we may think of the Lor^2 function as a

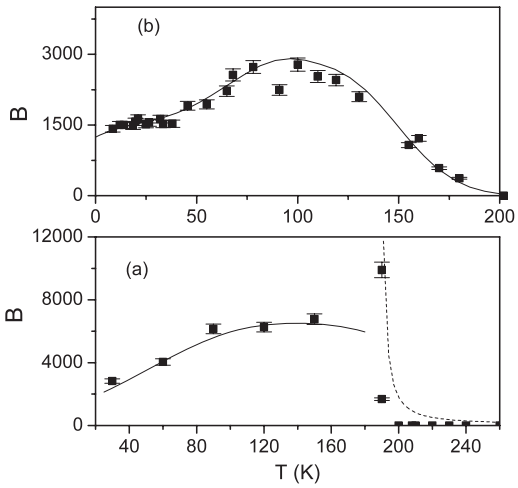

Figure 6. Coefficient B of the Lor^2 function versus temperature. (a) ZFC. Dashed line: equation (5). Continuous line: $B = B_1 \exp -|(T - 140\ \text{K})/110\ \text{K}|^{2.4}$. (b) ZFW. Continuous line: $B = B_1 \exp -|(T - 110\ \text{K})/50\ \text{K}|^{2.4} + B_2 \exp -|(T - 30\ \text{K})/60\ \text{K}|^{2.4}$.

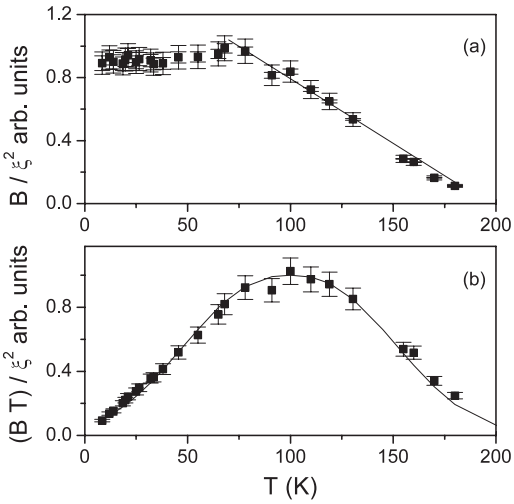

Figure 7. (a) Plot of B/ξ^2 versus temperature for the ZFW. (b) Plot of $C = BT/\xi^2$ versus temperature for the ZFW. Continuous line $C = \exp\{-|(T - 100\ \text{K})/65\ \text{K}|^{2.4}\}$.

type of Porod law as it also has the long Q dependence of Q^{-4}. In this case we may think of the coefficient B as a measure of the region surface. Under this assumption the ratio B/ξ^2 is proportional to the square of the magnetization of the interacting region interfaces. In figure 7(a) we observe that the values of B/ξ^2 for temperatures above 50 K decrease linearly with temperature and become zero at around $T_c = 188$ K. This behaviour shows that the magnetization at temperatures below 50 K is constant, then as the temperature increases the magnetization is reduced and becomes zero at T_c. The plot of TB/ξ^2 versus temperature shows a Gaussian type form (see figure 7(b)). This shows that the scaling of the SG state is quite complex.

Finally we need to assign some meaning to the coefficients A and B of the Lor and Lor^2 scattering laws. In order to be able to observe SANS from the sample it is necessary to have a magnetization difference between the entities giving the scattering law and the surrounding matrix (see equation (1)). Generally, both coefficients will depend on both the size of the objects and the magnetization difference, i.e. they could be written as $A, B \sim \xi^D |\mathbf{M}|^2$, where d is the dimensionality and M the magnetization difference, which could differ for A and B. Figure 7 is an attempt to reveal this type of dependence. The magnetization difference includes both possibilities of either an FM matrix or a paramagnetic one. An FM matrix, as has been indicated above, could be responsible for the Lor function (see figure 5), whereas the Lor^2 could arise from the SG state (see figure 7(b)). The difficulty for such an interpretation is that during ZFW we have no indication of the change of the FM state to paramagnetic around T_c (see figure 4). Also, an FM matrix would be expected to give a Q^{-2} scattering law, which is not observed. However, the question of the existence or not of a long-range order FM state can only definitely be answered by neutron scattering experiments at high Q values.

5. Conclusions

In this work the SG state of the amorphous alloy $Fe_{90}Nd_3Zr_7$ has been studied by SANS. Two types of experiments have been performed, one of cooling the sample from room temperature down to 10 K (ZFC) and the other of warming up to room temperature (ZFW). Though the parameters derived from these experiments are close in values, their functional form shows irreversibility between the ZFC and ZFW. The SANS scattering curves have been fitted by Lor and Lor + Lor^2 functions (equation (3)), the former functional form being applicable above $T_c = 188$ K and the latter below this temperature. In the case of Lor + Lor^2 the same correlation lengths were determined for both functions.

During ZFC a sharp type transition appears at $T_c = 188$ K, which can be scaled with a critical exponent $\nu = 1.4$. During ZFW no sharp transition is observed, but again the same scaling applies. This is indicative that below T_c there is no long-range FM order. As the temperature is lowered below the transition temperature the system breaks up into different regions with different exchange constants or $T_{c'}$s. Regions having $T_{c'}$ close to the sample temperature attempt to grow, but, through the interaction with adjacent regions having lower $T_{c'}$, break up again. It appears that there are two $T_{c'}$ distinct distributions, one centred around 140 K and the other around 30 K. The Lor^2 part of the scattering law has been attributed to the interfaces of the regions, whereas the Lor part to the core of the region as it attempts to undergo an FM transition. The possibility of the Lor scattering arising from an FM matrix cannot be totally excluded, but there is no concrete experimental evidence to support it. It is hoped that these results will stimulate interest in the calculation of the static correlation functions of these systems.

Acknowledgments

We would like to thank the British Council and the Greek General Secretariat of Research and Technology for financial

support and the SERC for the use of ISIS facilities. The contribution of Dr R Heenan and Dr S King during the experiments is appreciated.

References

[1] Binder K and Young A P 1986 *Rev. Mod. Phys.* **58** 801
[2] Maletta H, Aeppli G and Shapiro S M 1982 *Phys. Rev. Lett.* **49** 1490
[3] Motoya K, Shapiro S M and Muraoka Y 1983 *Phys. Rev.* B **28** 6183
[4] Nirera S and Matsubara F 2007 *Phys. Rev.* B **75** 144413
[5] Sherrington D and Kirkpatrick S 1975 *Phys. Rev. Lett.* **32** 1782
[6] Gabay M and Toulouse G 1981 *Phys. Rev. Lett.* **47** 201
[7] Perumal A, Srinivas V, Kim K S, Yu S G, Rao V V and Dunlap R A 2002 *Phys. Rev.* B **65** 06628
[8] Ryan D H, VaLierop J, Pumarol M E, Roseman M and Cadogen J M 2001 *Phys. Rev.* B **63** 140405
[9] Kaul S N, Siruguri V and Chandra G 1992 *Phys. Rev.* B **45** 12343
[10] Read D A, Hallam G C and Chirwa M 1989 *J. Magn. Magn. Mater.* **82** 83
[11] Babu P D and Kaul S N 1997 *J. Phys.: Condens. Matter* **9** 7189
[12] Perumal A, Shinivas V, Rao V V and Dunlap R A 2000 *Phys. Status Solidi* a **178** 783
[13] Mergia K, Messoloras S, Nicolaides G, Niarchos D and Stewart R J 1996 *J. Appl. Phys.* **76** 6380
[14] Aharony A and Pytte E 1983 *Phys. Rev.* B **27** 5872
[15] Aharony A, Imry Y and Ma S-K 1976 *Phys. Rev. Lett.* **37** 1367
[16] Grinstein G 1976 *Phys. Rev. Lett.* **37** 944
[17] Dominicis C de, Giardina I, Marinari E, Martin O C and Zuliani F 2005 *Phys. Rev.* B **72** 014443